Theor. Comput. Fluid Dyn. (2006) 20: 485–499
DOI 10.1007/s00162-006-0026-x

ORIGINAL ARTICLE

Olivier Pauluis · Dargan M. W. Frierson · Stephen T. Garner
Isaac M. Held · Geoffrey K. Vallis

The hypohydrostatic rescaling and its impacts on modeling of atmospheric convection

Received: 11 August 2005 / Accepted: 25 April 2006 / Published online: 5 October 2006

Abstract The atmospheric circulation spans a wide range of spatial scales, including the planetary scale (∼10,000 km), synoptic scale (∼2,000 km), mesoscale (∼200 km), and convective scales (<20 km). The wide scale separation between convective motions, responsible for the vertical energy transport, and the planetary circulation, responsible for the meridional energy transport, has prevented explicit representation of convective motions in global atmospheric models. Kuang et al. (Geophys. Res. Lett. 32: L02809, 2005) have suggested a way to circumvent this limitation through a rescaling that they refer to as Diabatic Acceleration and REscaling (DARE). We focus here on a modified version of the procedure that we refer to as hypohydrostatic rescaling. These two strategies are equivalent for inviscid and adiabatic flow in the traditional meteorological setting in which the vertical component of the Coriolis acceleration is ignored, but they differ when atmospheric physics is taken into account. It is argued here that, while the hypohydrostatic rescaling preserves the dynamics of the planetary scale circulation, it increases the horizontal scale of convective motions. This drastically reduces the computational cost for explicit simulation of hypohydrostatic convection in a global atmospheric model. A key question is whether explicit simulations of hypohydrostatic convection could offer a valid alternative to convective parameterization in global models. To do so, radiative–convective equilibrium is simulated with a high-resolution non-hydrostatic model using different model resolutions and values of the rescaling parameter. When the behavior of hypohydrostatic convection is compared with coarse-resolution simulations of convection, the latter set of simulations reproduce more accurately the result from a reference high-resolution simulation. This is particularly true for the convective velocity and cloud ice distributions. Scaling arguments show that hypohydrostatic rescaling increases the convective overturning time. In particular, this convective slowdown associated with the hypohydrostatic rescaling is more significant than the slowdown resulting from

Communicated by R. Klein.

O. Pauluis (✉)
Courant Institute of Mathematical Sciences, New York University,
251 Mercer Street, New York, NY 10012, USA
E-mail: pauluis@cims.nyu.edu

Dargan M. W. Frierson
Department of Geophysical Sciences, University of Chicago,
Chicago, IL, USA

Stephen T. Garner · Isaac M. Held
Geophysical Fluid Dynamics Laboratory/NOAA,
Princeton, NJ, USA

Geoffrey K. Vallis
Atmospheric and Oceanic Sciences Program,
Princeton University,
Princeton, NJ, USA

under-resolving the convective elements. These results cast doubt on the practical value of the hypohydrostatic rescaling as an alternative to convective parameterization.

Keywords Moist convection · General circulation of the atmosphere · Climate model

PACS 92.70.Np: Global climate modeling, 92.60.-e: Properties and dynamics of the atmosphere; meteorology, 92.60.hk: Convection, turbulence, and diffusion, 92.60.Ox: Tropical meteorology

1 Introduction

The representation of convective motions in global atmospheric models has always been a central issue in climate modeling, as the resolution in general circulation models (GCMs) is usually insufficient to explicitly simulate convective motions. In order to narrow the gap between convective and planetary scales, Kuang et al. [11, hereafter KBB] proposes using a rescaling strategy – Diabatic Acceleration and REscaling (DARE) – therefore making it possible to design a global model that also resolves the convective scale. The present paper discusses the hypohydrostatic rescaling (also called RAVE in KBB), which is a closely related alternative to DARE, and investigates whether hypohydrostatic simulations can reproduce the behavior of atmospheric convection.

The interaction between moist convection and the large-scale circulation is a central aspect of the tropical climate. At a fundamental level, the atmospheric circulation is a response to the differential heating of the Earth. The main energy source is associated with the absorption of solar radiation that occurs primarily at the surface and in the tropical regions, while the atmosphere is cooled through the emission of infrared radiation, mostly in the troposphere and at higher latitudes. The atmospheric circulation acts to balance this differential heating by transporting energy both in the vertical (from the surface to the upper troposphere) and horizontal (from Equator to Pole) directions. The vertical transport is dominated by moist convection, which occurs on scales comparable to the depth of the troposphere (10 km). In contrast, the horizontal transport is associated primarily with a planetary-scale circulation on a global scale (10,000 km), with a significant contribution from synoptic systems in mid-latitudes (2000 km). Because of various nonlinear mechanisms associated with advection, precipitation, and radiative transfer, these different scales continuously interact with each other.

That the vertical and horizontal atmospheric energy transports are dominated by processes occurring on very different scales has been a central limitation to our ability to simulate the climate system. Indeed, to this day, computing resources have limited GCMs to be run with a resolution of the order of 100 km, which is insufficient to explicitly represent the convective scale. Instead, GCMs must rely on so-called cumulus parameterization to determine the overall effects of convective systems on atmospheric temperature and humidity through a set of closure assumptions. Unfortunately, it is also known that a wide variety of mechanisms such as downdrafts, cold pool dynamics, mesoscale precipitation, vertical wind shear, mid-tropospheric humidity, and surface evaporation, affect the intensity and organization of deep convection. These mechanisms involve scales that are not represented in GCMs, and are usually not accounted for by convective parameterization. The necessary use of cumulus parameterization in the current generation of GCM is one of main sources of uncertainty in the prediction of future climate change.

In contrast, high-resolution Cloud System Resolving Models (CSRMs) have been designed to study the dynamics of atmospheric moist convection. CSRMs traditionally have a horizontal resolution of the order of 1–2 km, which is sufficient to explicitly simulate the processes associated with the organization of convection. They have been shown to be able to reproduce the observed behavior of convection much more closely than cumulus parameterizations [17]. The development of CSRMs was initially driven in the 1980s by studies of deep convection over limited areas [9,13]. They have been evaluated against various observational data sets (see for example [6,21]). Over time, the continuous increase in computing resources has greatly expanded their possible applications, both in terms of domain size and length of simulations [7,8,20]. While Tomita et al. [19] have reported performing a first global CSRM simulation, computational resources are still insufficient to simulate the long periods of time required for climate applications.

While a global CSRM might be available for climate simulations within the next decade, it might already be possible to take advantage of CSRMs to investigate scale interaction between convection and the large-scale circulation. Several strategies have been proposed to take advantage of CSRMs to improve climate simulations at reasonable computational cost. For example, Randall et al. [18] have suggested the use of CSRMs as a so-called super-parameterization in which explicit simulations of convection would replace the convective parameterization in a GCM. A second possibility lies in the results of Pauluis and Garner [15] who find that a CSRM with a coarse resolution on the order of 10–15 km, which is larger than most clouds, can nevertheless

reproduce the statistical behavior of convective systems. A third possibility is to use a rescaling approach, in which the model equations are modified, in order to change the scale at which convection takes place.

KBB have proposed a rescaling approach under the acronym DARE, in which one simulates a small, rapidly rotating planet and with enhanced diabatic forcings. This reduces the scale of the planetary-scale circulation while leaving the convective scale unchanged. The increased rotation rate and strength of the forcing are needed to ensure the similarity of the planetary-scale circulation. An alternative, and perhaps simpler method, that we refer here to as the deep Earth rescaling, involves reducing the gravitational acceleration, thereby increasing the scale height of the atmosphere and the horizontal scale of convection, while leaving the planetary-scale circulation unaffected. The simplest approach from a modeling point of view is provided by what we refer to as the hypohydrostatic rescaling (also called RAVE in KBB) in which one rescales the vertical acceleration.

Section 2 describes these rescaling strategies, and shows that these three approaches are mathematically equivalent in a dry atmosphere. Their use reduces the scale separation between the convective scales and the planetary scales. Section 3 compares the behavior of hypohydrostatic and coarse simulations of radiative–convective equilibrium. Simulations with various resolutions and rescaling parameters are compared with a high-resolution reference simulation. The goal here is to assess whether coarse and hypohydrostatic models can reproduce the statistical behavior of convection in high-resolution simulations, and therefore determine whether such models can successfully replace traditional convective parameterizations.

2 Convective rescaling

In this section, we discuss how the scale separation between convection and the planetary-scale circulation can be artificially modified, either by reducing the Earth's size (DARE), or increasing the horizontal size of convective systems by either changing the depth of the troposphere (Deep Earth approach) or changing the equation of motions (the hypohydrostatic approximation). These three approaches are shown to be mathematically equivalent for a dry atmosphere. This section is primarily an extension and clarification of the arguments presented in KBB. Some of the points here have already been made by these authors in various conferences or during our discussions with them.

2.1 Equation of motions

The equations of motion for a compressible fluid in Cartesian coordinates in a rotating reference frame are

$$\frac{\mathrm{d}w}{\mathrm{d}t} = -g - \rho^{-1}\frac{\partial p}{\partial z} + F_z \tag{1}$$

$$\frac{\mathrm{d}\mathbf{V}_H}{\mathrm{d}t} = -\rho^{-1}\nabla_H p - f\mathbf{V}_H^o + \mathbf{F}_H \tag{2}$$

$$C_p\frac{\mathrm{d}T}{\mathrm{d}t} + \rho^{-1}\frac{\mathrm{d}p}{\mathrm{d}t} = Q \tag{3}$$

$$\frac{\partial \rho}{\partial t} + \nabla\cdot(\rho\mathbf{V}_H) + \frac{\partial(\rho w)}{\partial z} = 0 \tag{4}$$

$$p = \rho RT\,, \tag{5}$$

where $\frac{\mathrm{d}}{\mathrm{d}t} = \frac{\partial}{\partial t} + \mathbf{V}_H\cdot\nabla + w\frac{\partial}{\partial z}$ is the Lagrangian derivative, $\mathbf{V}_H = (u, v)$ is the horizontal velocity, w is the vertical velocity, T is the temperature, ρ is the density, p is the pressure, g is the gravitational acceleration, $f = 2\Omega\sin\theta$ is the Coriolis parameter, with Ω being the Earth's rotation rate, and θ the latitude, $\mathbf{V}_H^0 = (-v, u)$ denotes the orthogonal component to the horizontal wind, C_p is the sensible heat at constant pressure, R is the ideal gas constant for dry air. $\mathbf{F}_H = (F_x, F_y)$ and F_z are, respectively, the horizontal and vertical acceleration due to sub-grid-scale processes (i.e. molecular or turbulent diffusion), Q is the external heating. For simplicity, we assume here that the rotation axis and gravity vector are aligned.

In the absence of motion, the vertical momentum equation reduces to the hydrostatic balance

$$\frac{\partial p}{\partial z} = -\rho g \tag{6}$$

between gravity and the vertical pressure gradient. For circulations where the aspect ratio H/L is small, where H and L are the vertical and horizontal extent of the circulation, the Lagrangian advection of vertical velocity is small. In this case, hydrostatic balance offers a very good approximation for the vertical momentum equation. In the atmospheric sciences, the system of equations in which the vertical momentum equation (1) has been replaced by the hydrostatic balance (6) is known as the primitive equations. In so doing, one has replaced a prognostic equation by a diagnostic equation, so the system loses one degree of freedom corresponding to vertically propagating sound waves (horizontally propagating Lamb waves are still part of the solution). The use of the primitive equations in geometric coordinates is made difficult by the need to solve for pressure and density simultaneously. However, this problem can be avoided by using the hydrostatic pressure as the vertical coordinates (see Lorenz 1965 for a discussion). The primitive equations in pressure (or pressure-like) coordinates have been widely used for the modeling of large-scale flows, and are the basis for most climate models.

One of the main limitations of the primitive equations lies in how they handle the kinetic energy of convective motions. The kinetic energy tendency in the primitives equation can be obtained by adding equation (2) multiplied by equation $\rho \mathbf{V}_H$ and Eq. (6) multiplied by ρw:

$$\frac{1}{2}\frac{\partial(\rho|\mathbf{V}_H|^2)}{\partial t} + \nabla_H \cdot \left(\mathbf{V}_H \frac{\rho|\mathbf{V}_H|^2)}{2}\right) + w\frac{\partial}{\partial_z}\left(\mathbf{w}\frac{\rho|\mathbf{V}_H|^2)}{2}\right) = -gw - \mathbf{V}_H \cdot \nabla_H p - w\frac{\partial p}{\partial z} + \mathbf{V}_H \cdot \mathbf{F}_H + wF_z \tag{7}$$

The kinetic energy in the primitive equations is thus $ke_{\mathrm{hyd}} = \frac{1}{2}|\mathbf{V}|_H^2$; it only accounts for the contribution of the horizontal motions and omits the vertical component. For planetary- or synoptic-scale circulations, the vertical velocity is much smaller than the horizontal velocity, and its contribution to the kinetic energy is negligible. This is not the case for convective motions for which the use of the primitive equations leads to unrealistic values of the vertical velocity. In fact, analytic solutions of the primitive equations in a convectively unstable atmosphere yield infinite growth rate for short horizontal wavelengths.

When using the full vertical momentum equation, the kinetic energy takes its traditional form: $ke = \frac{1}{2}(|\mathbf{V}|_H^2 + w^2)$. A non-hydrostatic component to the pressure field must exert mechanical work to accelerate convective updrafts. This in particular prevents infinite growth rate in convective instability. In addition, a large fraction of the vertical kinetic energy in atmospheric convection motions is either dissipated through a turbulent energy cascade, or radiated away by gravity waves. As a consequence, the amount of kinetic energy that ends up in horizontal motion will be smaller in a non-hydrostatic model than in an equivalent model based on the primitive equations. A proper representation of convective motions is a key motivation for switching from hydrostatic to non-hydrostatic models when the grid resolution becomes comparable to the depth of the troposphere.

2.2 The hypohydrostatic, DARE and Deep Earth rescalings

In order to better understand the interactions between the convective motions and the planetary-scale circulation, one needs a model that can resolve the convective scale while covering a large enough domain to encompass the entire globe. Computing resources have so far been insufficient to do this on a routine basis, but a few research centers have been able to run a global model with resolution of 10 km or less. The hypohydrostatic rescaling discussed here is an alternative to the DARE and Deep Earth approaches, and offers a method to change the scale separation between convection and the planetary scales. This can be used to investigate the nature of the interaction between convection and the large-scale circulation, to test and develop global non-hydrostatic models, and possibly as an alternative to convective parameterizations.

Hypohydrostatic rescaling. In the hypohydrostatic equation, the inertia of vertical motion is increased. To do so, the vertical momentum equation (1) is replaced by:

$$\alpha^2 \frac{\mathrm{d}w}{\mathrm{d}t} = -g - \rho^{-1}\frac{\partial p}{\partial z} + F_z \tag{8}$$

with $\alpha \geq 1$. As discussed in the Appendix, the implementation of the hypohydrostatic approximation may also require a rescaling of the sub-grid-scale viscosity $\mathbf{F}$, but beside this, no other changes are required in the model. The case $\alpha = 1$ corresponds to the compressible Navier–Stokes equations.

DARE. KBB have proposed the DARE method. Here, rather than modifying the behavior of convective motions, the size of the Earth and the length of the day are reduced by a factor β, while the depth of the atmosphere is left unchanged:

$$t, x, y|_D \to \frac{t}{\beta}, \frac{x}{\beta}, \frac{y}{\beta} \tag{9}$$

$$z|_D, g \to z, g \tag{10}$$

$$f_D, \mathbf{F}, Q|_D \to \beta f, \beta \mathbf{F}, \beta Q \tag{11}$$

While the DARE method requires more delicate adjustment within a model, it provides a physical analog in that it is still based on the compressible Navier–Stokes equations.

Deep Earth rescaling. Rather than reducing the size of the Earth, one can increase the depth of the atmosphere. The pressure scale height of an isothermal atmosphere is given by $H_p = \frac{RT}{g}$. In Deep Earth simulations, the gravitational acceleration g and the height of the atmosphere is increased:

$$g|_g \to \frac{g}{\gamma} \tag{12}$$

$$z|_g \to \gamma z \tag{13}$$

$$x, y, t, f, \mathbf{F}, Q|_g \to x, y, t, f, \mathbf{F}, Q \tag{14}$$

The size of Earth, its rotation rate and the diabatic forcings Q are constant. Similar to DARE, the deep Earth rescaling solves the compressible Navier–Stokes equations, and thus has a physical analog. If density and hydrostatic pressure are kept constant, this would imply that the mass of the total atmosphere increases proportionally to γ. It is also possible to keep the atmospheric mass constant, which would require one to scale the pressure and density as γ^{-1}. This choice does not affect the dynamical behavior, as the changes in the pressure and density terms cancel each other in the momentum equations, but it impacts on the physical parameterizations used to compute Q and $\mathbf{F}$ in atmospheric models.

The hypohydrostatic rescaling, DARE, and the Deep Earth rescaling are mathematically equivalent: any solution obtained for one rescaling method corresponds exactly to one solution under another rescaling. More precisely, if $\mathbf{V}_{H,\alpha}, w_\alpha, T_\alpha, \rho_\alpha, p_\alpha(x_\alpha, y_\alpha, z_\alpha, t_\alpha)$ is a solution of the hypohydrostatic equations for a forcing $\mathbf{F}_{H\alpha}, F_z\alpha, Q_\alpha(x_\alpha, y_\alpha, z_\alpha, t_\alpha)$, then a solution for the DARE problem is

$$\beta = \alpha \tag{15}$$

$$t_D, x_D, y_D = \frac{t_\alpha}{\alpha}, \frac{x_\alpha}{\alpha}, \frac{y_\alpha}{\alpha} \tag{16}$$

$$z_D = z_\alpha \tag{17}$$

$$u_D, v_D, T_D, p_D, \rho_D(x_D, y_D, z_D, t_D) = u_\alpha, v_\alpha, T_\alpha, p_\alpha(x_\alpha, y_\alpha, z_\alpha, t_\alpha) \tag{18}$$

$$w_D(x_D, y_D, z_D, t_D) = \alpha w_\alpha(x_\alpha, y_\alpha, z_\alpha, t_\alpha) \tag{19}$$

$$f_D, Q_D, \mathbf{F}_{HD}, F_{zD}(x_D, y_D, z_D, t_D) = \alpha f_\alpha, \alpha Q_\alpha, \alpha \mathbf{F}_{H\alpha}, \alpha F_{z\alpha}(x_\alpha, y_\alpha, z_\alpha, t_\alpha)\,. \tag{20}$$

Similarly, a solution for the Deep Earth is given by

$$\gamma = \alpha \tag{21}$$

$$t_g, x_g, y_g = t_\alpha, x_\alpha, y_\alpha \tag{22}$$

$$z_g = \alpha z_\alpha \tag{23}$$

$$u_g, v_g, T_g, p_g, \rho_g(x_g, y_g, z_g, t_g) = u_\alpha, v_\alpha, T_\alpha, p_\alpha, \rho_\alpha(x_\alpha, y_\alpha, z_\alpha, t_\alpha) \tag{24}$$

$$w_g(x_g, y_g, z_g, t_g) = \alpha w_\alpha(x_\alpha, y_\alpha, z_\alpha, t_\alpha) \tag{25}$$

$$f_g, Q_g, \mathbf{F}_{HD}, F_{zg}(x_g, y_g, z_g, t_g) = f_\alpha, Q_\alpha, \mathbf{F}_{H\alpha}, F_{z\alpha}(x_\alpha, y_\alpha, z_\alpha, t_\alpha)\,. \tag{26}$$

Because of these equivalences, it is only necessary to analyze the impact of one of these strategies. The rest of the paper will focus on the hypohydrostatic equation, as this is the easiest to implement in a numerical model, but the discussion can be easily extended to DARE and Deep Earth.

2.3 Hydrostatic and non-hydrostatic behaviors

Consider now the behavior of the hypohydrostatic system for a a given value of α. For the large-scale circulation, i.e. a circulation characterized by a sufficiently large aspect ratio, the primitive equations should still constitute a good approximation. In this case, the hypohydrostatic rescaling does not affect the behavior of the solution. It will however affect the horizontal scale at which non-hydrostatic effects become noticeable. Indeed, the kinetic energy under the hypohydrostatic equations is given by $ke_\alpha = \frac{1}{2}(|\mathbf{V}|_H^2 + \alpha^2 w^2)$. The primitive equations and the compressible Navier–Stokes equations correspond to $\alpha = 0$ and $\alpha = 1$, respectively. The hypohydrostatic approximation increases the contribution of the vertical component, and therefore reduces the range of scales at which the hydrostatic approximation is valid.

The continuity equation implies that the vertical velocity varies at least as the aspect ratio: [1]

$$w \approx \frac{H}{L}|\mathbf{V}|_H \,. \tag{27}$$

In the compressible Navier–Stokes equations, the contribution of the vertical kinetic energy becomes comparable to the horizontal kinetic energy for aspect ratios on the order of unity. This corresponds to the transition between hydrostatic and non-hydrostatic behavior. Under the hypohydrostatic approximation, this transition will occur at larger horizontal scales, corresponding to an aspect ratio $\frac{H}{L}\ \alpha^{-1}$. Garner et al. [5] analyze in greater detail the impact of the hypohydrostatic equation on the planetary-scale circulation. This paper focuses primarily on the behavior of convective motions.

For purely convective circulations, i.e., for a horizontally uniform forcing and no rotation ($f = 0$), a solution of the hypohydrostatic equation is also a solution of the compressible Navier–Stokes equations after the transformation:

$$t, x, y = \frac{t_\alpha}{\alpha}, \frac{x_\alpha}{\alpha}, \frac{y_\alpha}{\alpha} \tag{28}$$

$$z = z_\alpha \tag{29}$$

$$u, v, T, p, \rho(x, y, z, t) = u_\alpha, v_\alpha, T_\alpha, p_\alpha(x_\alpha, y_\alpha, z_\alpha, t_\alpha) \tag{30}$$

$$w(x, y, z, t) = \alpha w_\alpha(x_\alpha, y_\alpha, z_\alpha, t_\alpha) \tag{31}$$

$$Q, \mathbf{F}_H, F_z(x, y, z, t) = \alpha Q_\alpha, \alpha \mathbf{F}_{H\alpha}, \alpha F_{z\alpha}(x_\alpha, y_\alpha, z_\alpha, t_\alpha) \,. \tag{32}$$

This implies that hypohydrostatic convection behaves exactly as non-hydrostatic convection with: (1) the horizontal scale stretched by a factor α; (2) vertical velocity weaker by a factor α; (3) the convective overturning time increased by a factor α; and (4) the convective heat transport reduced by a factor α. The latter point implies that, if hypohydrostatic convection is forced by imposing a radiative cooling throughout the troposphere (and compensating it by a surface energy flux), it will behave like atmospheric convection but forced with radiative cooling enhanced by a factor α. As the hypohydrostatic rescaling increases the horizontal scale of convective motions, it also increases the convective overturning time.

The behavior of the hypohydrostatic rescaling is different for the planetary and convective scales. Indeed, for small aspect ratios, the vertical velocity is independent of the rescaling parameter. However, for convective motions, with an aspect ratio on the order of unity, Eq. (31) indicates that the vertical velocity should scale as α^{-1}. This different behavior at the planetary and convective scales is precisely the intent of the hypohydrostatic rescaling, as it corresponds to an increase of the horizontal extent of convective motions without modifying the large-scale dynamics.

2.4 Spherical coordinates

Equations (1–5) are written in Cartesian coordinates and assume that the axis of rotation is aligned with the gravitational acceleration. In order to study of the planetary-scale circulation, they must be modified by using spherical coordinates and by allowing for a horizontal component of the rotation. While this paper focuses on the convective scales for which the system (1–5) is perfectly adequate, we briefly address how the rescaling strategies should be recast in studies of the planetary circulation.

[1] This scaling is an upper bound. Indeed, for geostrophic motions in a stratified fluid, the vertical velocity scales as $w \approx Ro\frac{H}{L}|\mathbf{V}|_H$, where $Ro = |\mathbf{V}|_H f/L$ is the Rossby number (see [16]).

First, it should be stressed that the DARE and deep Earth rescaling are always equivalent. Comparing equations (16–17) and (22–23) indicates that, in order to transform a DARE solution into a solution under the Deep Earth rescaling, it is sufficient to renormalize the time and spatial units through

$$t_g, x_g, y_g, z_g = \alpha t_D, \alpha x_D, \alpha y_D, \alpha z_D \,. \tag{33}$$

In particular, as this transformation is independent of the direction, solutions remain equivalent even in the spherical geometry or for different direction of the axis of rotation.

The problem here is to formulate the hypohydrostatic rescaling so that it remains consistent with DARE and the deep Earth rescaling. To this effect, changes must be made to terms involving the horizontal component of the Earth's rotation, and to the metric terms. Consider first the situation where the axis of rotation has a horizontal component $f_H = 2\Omega\cos\theta$ pointing in the y-direction. This results in an acceleration in the x-direction given by $-f_H w$, and a vertical acceleration equal to $f_H u$. In the hypohydrostatic relationship, the acceleration in the x-direction must be rescaled as $-\alpha f_H w$ while a term $\alpha f_H u$ must be added to the right-hand side of (8). This ensures the equivalence of the solutions of the hypohydrostatic rescaling with solutions of the DARE and Deep Earth rescaling.

In spherical coordinates, metric terms are included in the velocity tendency for the three-dimensional velocity to account for the variations of the local vector basis. The terms that should added on the right-hand side of Eqs. (1) and (2) are: in the zonal direction $\frac{uv}{r}\tan\theta - \frac{vw}{r}$, where r is the radius; in the meridional direction $-\frac{u^2}{r}\tan\theta - \frac{uw}{r}$; and in the vertical direction $\frac{u^2+v^2}{r}$. In atmospheric science, it is common to make use of the thin-shell approximation in which the radius r used in the metric terms is replaced by the (mean) radius of Earth a. Within this approximation, the hypohydrostatic rescaling can be made equivalent to DARE and the deep Earth rescaling as long as the metric terms are replaced by following terms: in the zonal direction $\frac{uv}{a}\tan\theta - \alpha\frac{vw}{a}$; in the meridional direction $-\frac{u^2}{a}\tan\theta - \alpha\frac{uw}{a}$; and in the vertical direction $\alpha\frac{u^2+v^2}{a}$. [The latter is to be added to the right-hand side of (8).] Without making the thin-shell approximation, the equivalence can be obtained by replacing the radius of the Earth a by $a + \alpha z$ in the metric terms, where $z = r - a$ is the height above the sea level.

2.5 Atmospheric physics

In order to solve the compressible Navier–Stokes equations, atmospheric models must also determine the forcing terms $\mathbf{F}$ and Q. These account for a wide range of physical processes ranging from turbulence, energy and momentum exchange with the Earth's surface, phase transitions for water, cloud microphysics, precipitation, and radiative transfer. While the three rescalings in Sect. 2.2 are mathematically equivalent for the compressible Navier–Stokes equation with prescribed forcings, they do differ as far as the implementation of the physical processes is concerned. The hypohydrostatic rescaling does not modify the diabatic forcing, so that the standard physical parameterizations can be used directly. However, for high-resolution simulations, an isotropic turbulence closure scheme must be modified to ensure consistency with the rescaling, as discussed in the Appendix.

Cloud microphysics plays a central role in CSRM and requires particular attention in the rescaling. The microphysical parameterizations usually separate condensed water into a number of bulk types, such as cloud water, cloud ice, rain droplets, snow, graupel and hail. Microphysical schemes determine the various conversion rates between these different species as well as the relative velocity of falling precipitation. A direct application of the hypohydrostatic rescaling implies that conversion rates and terminal velocity v_T remain unchanged

$$v_{T,\alpha} = v_T \,. \tag{34}$$

In this case, the microphysical processes are rescaled consistently with the vertical velocity and time for the large-scale circulation. In DARE, KBB rescale the terminal velocity with the same factor as used for the diabatic terms, which lead to the same result. We believe that the rescaling of the mircophysical processes consistently with the large-scale circulation should be favored for climate simulations in order to properly account for cloud–radiative feedbacks.

An alternative is to consider microphysical processes as an intrinsic part of convective systems. In particular, this requires one to rescale the conversion rates and terminal velocity using (29–32):

$$v_{T,\alpha} = \alpha^{-1} v_T \tag{35}$$

This conserves the ratio between the precipitation speed and vertical velocity in the updrafts. This would ensure, among other things, that the precipitation efficiency, i.e. the fraction of the precipitation water that reaches the ground, would not be affected by the rescaling in the convective regime. Using the DARE approach (or Deep Earth for that matter) while leaving the vertical velocity unchanged corresponds to this second option.

The main issue here lies in the fact that microphysics plays a significant role both at the convective and planetary scales. Because the rescalings affect the timescales of convective and planetary circulations differently, it is not possible to rescale the microphysical processes in a way that is consistent both with the small and large scale processes. Given the importance of cloud–radiative feedbacks, the priority should be given to the consistency with the large-scale processes.

3 Numerical simulations

3.1 Model and experiment

While the transformations (29–32) indicate that the behavior of hypohydrostatic convection is mathematically similar to atmospheric convection, they differs in that the former is significantly slower. A key question is whether, despite these differences, hypohydrostatic convection could be used to replace standard convective parameterizations in global models. To answer this question, a set of numerical simulations is used here to determine whether hypohydrostatic simulations can reproduce the statistical behavior of convection by comparing them with results from fine- and coarse-resolution simulations.

Radiative–convective equilibrium (RCE) is an idealized problem in which a horizontally uniform atmosphere is destabilized by a combination of heating at the Earth's surface and radiative cooling throughout the troposphere. Convective motions continuously grow, develop and decay, so that a statistical equilibrium can be established in which the differential heating is balanced by a convective energy transport. RCE can be thought of as the atmospheric analog to Rayleigh–Benard convection in which the energy sink at the upper boundary has been replaced by radiative cooling. It is however a much more complex problem due to the specific aspects of atmospheric convection associated with, among other things, phase transition, cloud microphysics, and radiative transfer.

Here, a RCE experiment is set up by using a doubly periodic atmospheric domain, heated by energy exchange with an ocean surface at a constant temperature of 301.15 K. Radiative heating and cooling rates are obtained through the Geophysical Fluid Dynamics Laboratory (GFDL) Flexible Modeling System radiation package [1,4], which uses the full cloud field. In addition, the horizontally averaged wind is relaxed with a timescale of 2, 500 s toward a reference wind profile horizontally prescribed by:

$$\overline{u_r}(z) = z\frac{\partial \overline{u}}{\partial z} \quad \text{for } z < 5000\,\text{m} \tag{36}$$

$$\overline{u_r}(z) = 5000\frac{\partial \overline{u}}{\partial z} \text{ elsewhere.} \tag{37}$$

$$\overline{v_r} = 0 \tag{38}$$

This imposes a constant shear in the lower 5,000 m of the domain, while keeping the horizontal wind constant above it. Wind shear has a strong impact on the organization of convection, and two set of simulations are performed, the first one with a weak shear $\frac{\partial \overline{u}}{\partial z} = 0.001\,s^{-1}$, in which convection is not organized, and the second with a strong shear $\frac{\partial \overline{u}}{\partial z} = 0.003\,s^{-1}$, which produces organized convection.

The model used here is the Zetac model developed at the Geophysical Fluid Dynamics Laboratory (GFDL) through a collaboration between Steve Garner, Olivier Pauluis, Chris Kerr, and Isidoro Orlanski. It is composed of three main components: (1) a compressible dynamical core, which solves the equation of motion for moist air, (2) a bulk microphysical parameterization that determines the conversion rates of the different types of water, and the associated latent heat release, and (3) a set of physical parameterizations shared with the GFDL climate model [1]. The dynamical core solves the fully compressible Navier–Stokes equation, using a time-splitting technique, with a long time step for advection and physics and a shorter time step for sound and gravity waves. Advective tendencies are obtained by using the Piecewise Parabolic Method (PPM) in all three directions for all variables [2]. Further discussion of the numerical aspects of the model can be found in the Appendix of Pauluis and Garner [15].

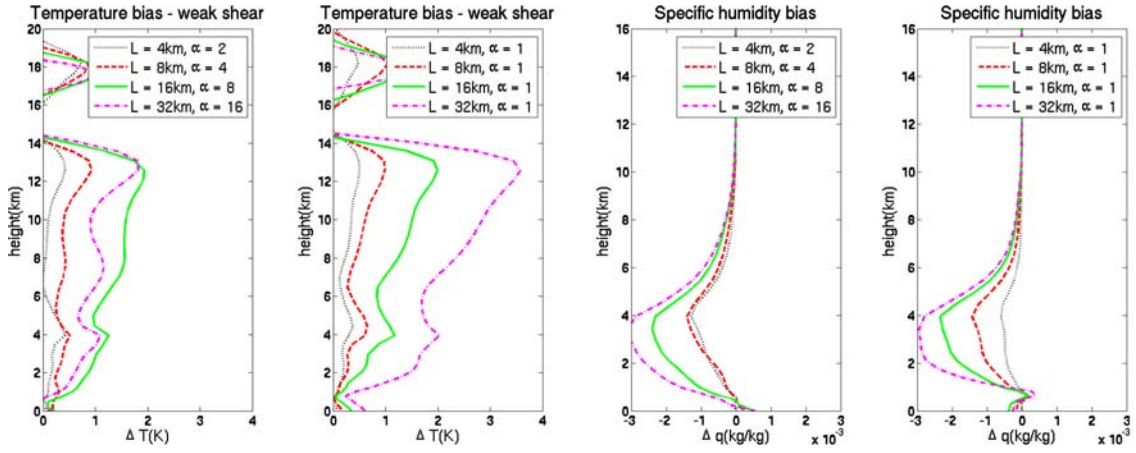

Fig. 1 Temperature and humidity biases in the weak-shear simulations. Bias here is the difference with the reference simulation ($\Delta x = 2\,\text{km}$, $\alpha = 1$). *First panel*: cloud water for the hypohydrostatic simulations. *Second panel*: the same for the coarse resolutions. *Third panel*: cloud ice for the hypohydrostatic simulations. *Fourth panel*: the same for the coarse-resolution simulations

Physical parameterizations are required to determine the momentum and diabatic forcing terms (**F** and Q terms in (1–5). In atmospheric convection, water vapor plays a crucial role, through condensation, re-evaporation, precipitation and water loading. In a CSRM such as Zetac, these are accounted for through a microphysical parameterization. Here, that of Lin et al. [12], with subsequent modifications by Lord et al. [14], and Krueger et al. [10] is used. It separates condensed water into five different species – cloud water, cloud ice, rain water, snow and graupel – and is used to compute the transformation rate between the different water types, as well as the corresponding temperature change. Turbulent mixing and viscosity is handled through a simple isotropic turbulent kinetic energy scheme similar to that of Klemp and Whilelmson [9]. In the Appendix, it is shown that the hypohydrostatic rescaling requires one to modify the turbulent closure scheme for energy consistency. The surface fluxes are obtained by using a Monin–Obhukov similarity theory. A sponge layer at the upper boundary damps vertically propagating sound and gravity waves. No parameterization for either shallow or deep convection has been used.

The model simulates convection on a three-dimensional domain, periodic in the horizontal directions. All simulations use a $50\times50\times60$ grid with uniform resolution in the horizontal and a stretch grid in the vertical. The vertical resolution ranges from 100 m near the ground to 700 m at the top (25 km). For each value of the wind shear, a reference simulation is performed with horizontal resolution $\Delta x = 2\,\text{km}$, and $\alpha = 1$. Four hypohydrostatic simulations with ($\Delta x = 4\,\text{km}$, $\alpha = 2$), ($\Delta x = 8\,\text{km}$, $\alpha = 4$), ($\Delta x = 16\,\text{km}$, $\alpha = 8$), ($\Delta x = 32\,\text{km}$, $\alpha = 16$), are compared with the results from coarse-resolution simulations with ($\Delta x = 4\,\text{km}$, $\alpha = 1$), ($\Delta x = 8\,\text{km}$, $\alpha = 1$), ($\Delta x = 16\,\text{km}$, $\alpha = 1$), ($\Delta x = 32\,\text{km}$, $\alpha = 1$). Computational costs for the hypohydrostatic and coarse runs are the same for the same model resolution. The combination of resolution and α in the hypohydrostatic runs is such that, under the transformation (29–32), the simulations should behave similarly to a simulations with $\Delta x = 2\,\text{km}$ and $\alpha = 1$ where the diabatic forcings (radiative cooling, surface energy fluxes and diffusion) have been accelerated by a factor α. Hence, the alpha runs can alternatively be viewed as evaluating the impacts of increased diabatic cooling on convection. The simulations are integrated for a period of 16 days, with the analysis performed on the last 8 days of the simulations. While 16 days is possibly too short for the model to reach full radiative–convective equilibrium, the initial conditions were obtained from a two-month integration with a 2 km resolution, and were already fairly close to the radiative–convective equilibrium state.

3.2 Results

Figures 1 and 2 show the bias in the horizontal mean temperature and humidity for the weak- and strong-shear cases. The bias here is the difference between a given simulation and the reference case ($\Delta x = 2\,\text{km}$, $\alpha = 1$). The α and coarse runs exhibit similar features: a slight moist bias near the surface, a pronounced dry bias in the free troposphere above the boundary layer, and a tropospheric deep warm bias. This behavior is similar to that observed in the coarse-resolution simulations of Pauluis and Garner [15]. For the same computational cost,

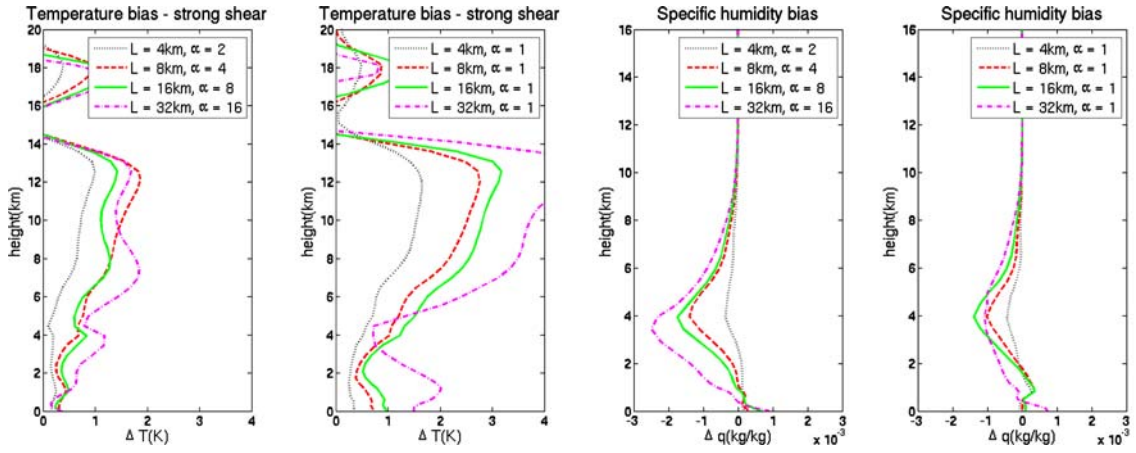

Fig. 2 Temperature and humidity biases in the strong-shear simulations. Bias here is the difference with the reference simulation ($\Delta x = 2\,\text{km}$, $\alpha = 1$). *First panel*: cloud water for the hypohydrostatic simulations. *Second panel*: the same for the coarse resolutions. *Third panel*: cloud ice for the hypohydrostatic simulations. *Fourth panel*: the same for the coarse-resolution simulations

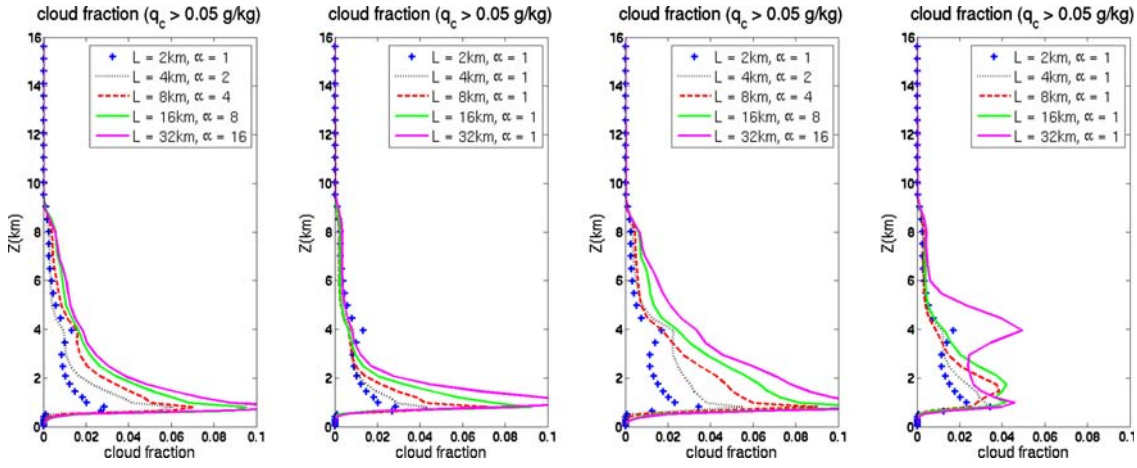

Fig. 3 The cloud water fraction is defined as the fraction of grid points at each level with $q_c > 0.05\,\text{g/kg}$. *First panel*: cloud water fraction for the hypohydrostatic simulations with weak shear. *Second panel*: the same for the coarse resolutions. *Third panel*: cloud water fraction for the hypohydrostatic simulations with strong shear. *Fourth panel*: the same for the coarse-resolution simulations

comparing the coarse and hypohydrostatic runs, the α rescaling reduces the temperature bias, but increases the error in the moisture field.

In radiative–convective equilibrium, the low-level humidity is determined by a balance between subsidence drying and moistening by shallow convection. Pauluis and Garner [15] argue that a lack of resolution prevents shallow overturning and inhibits the mixing of low clouds with the environment. This explains the behavior of the coarse-resolution experiment. The α experiments are such that the α rescaling corrects for the grid anisotropy so that the rescaled grid matches that of the reference case. However, the convective scalings (29–32) indicate that convective overturning time is also reduced by a factor α. Hence, despite the fact that the α rescaling corrects for the grid anisotropy, it also reduces the mixing between the planetary boundary layer and the lower troposphere.

The cloud water distributions in Fig. 3 show an excess of low-level cloud water at coarse resolution and large α. A lack of overturning in shallow convection prevents the mixing and dissipation of the shallow clouds. Arguably, even the 2 km resolution in the reference simulation is probably insufficient to capture the behavior of shallow convection accurately. The lack of convergence for shallow convection is one of the most stringent limitations of the coarse resolution and hypohydrostatic simulations in a climate regime, as poor representation of low-level clouds and water vapor have a very large impact on the radiative transfer. A positive aspect here lies in the fact that the coarse runs in the strong-shear case do a better job at capturing the low-level cloud

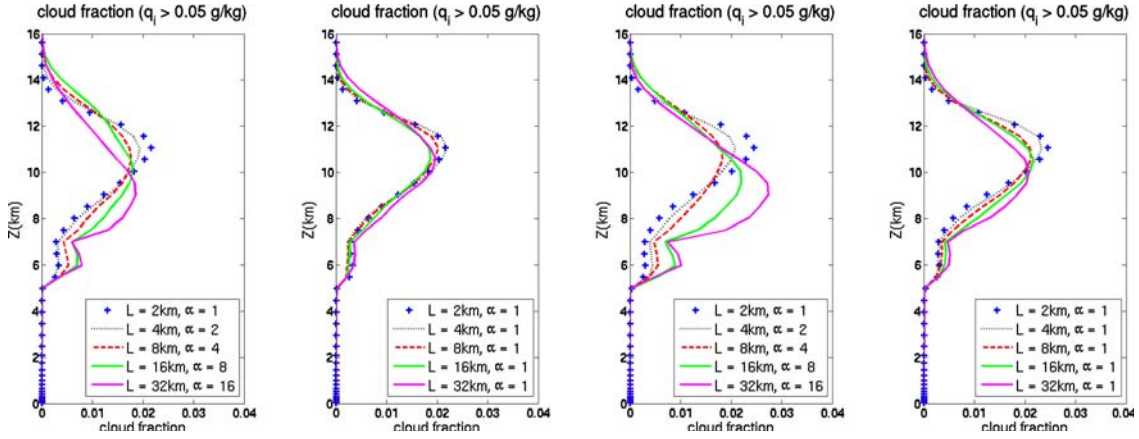

Fig. 4 The cloud ice fraction is defined as the fraction of grid points at each level with $q_i > 0.05$ g/kg. *First panel*: cloud ice fraction for the hypohydrostatic simulations with weak shear. *Second panel*: the same for the coarse resolutions. *Third panel*: cloud ice fraction for the hypohydrostatic simulations with strong shear. *Fourth panel*: the same for the coarse-resolution simulations

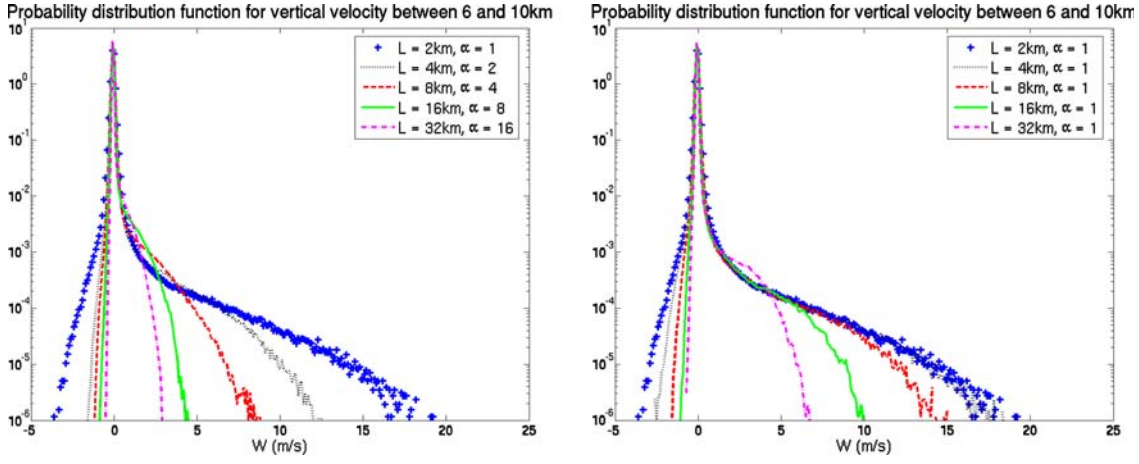

Fig. 5 Vertical velocity distribution function between 6 and 10 km in the weak shear experiment. *Left panel*: hypohydrostatic runs, *right panel*: coarse-resolution runs

distribution. These runs also exhibit the best convergence for tropospheric water vapor. While this is limited to the strong shear case, this indicates that a better representation of low-level mixing should produce an improvement in both cloud fraction and water vapor distribution.

Figure 4 shows the vertical profile of cloud ice. The ($\Delta x = 4$ km, $\alpha = 2$) and ($\Delta x = 8$ km, $\alpha = 4$) runs capture both the amplitude and magnitude of the peak in the cloud ice fraction, indicative of the main detrainment level for cirrus clouds. The ($\Delta x = 16$ km, $\alpha = 8$) run still does a reasonable job in the weak-shear case, but misses the peak distribution by more than 2 km in the strong-shear case. The ($\Delta x = 32$ km, $\alpha = 16$) run cannot capture the cloud ice distribution even in the weak-shear case. While the hypohydrostatic runs produce a satisfactory result for intermediate value of α, the coarse-resolution simulations outperform them at comparable resolution. The ($\Delta x = 4$ km, $\alpha = 1$) run is a very close match to the reference run, and the ($\Delta x = 8$ km, $\alpha = 1$) ($\Delta x = 16$ km, $\alpha = 1$) runs remain very good. Even the ($\Delta x = 32$ km, $\alpha = 1$) runs reproduce the cloud ice distribution more accurately than the ($\Delta x = 16$ km, $\alpha = 8$) run. The ability to reproduce the high-level cloud cover is a very promising feature of the low-α coarse-resolution simulations. The robust behavior of the high-level clouds is related to the model's ability to reproduce the vertical velocities of deep convection. Figures 5 and 6 show the probability distribution functions of the vertical velocity between 6 and 10 km for the weak and strong shear cases respectively. The rescaling parameter has a large impact on the vertical velocity. For instance, the peak velocity is about three times smaller in the ($\Delta x = 8$ km, $\alpha = 4$) run than in the reference simulations. The weakening of the updraft velocity is associated with an increased probability for weak velocities. For convective motions, the hypohydrostatic rescaling for vertical velocity

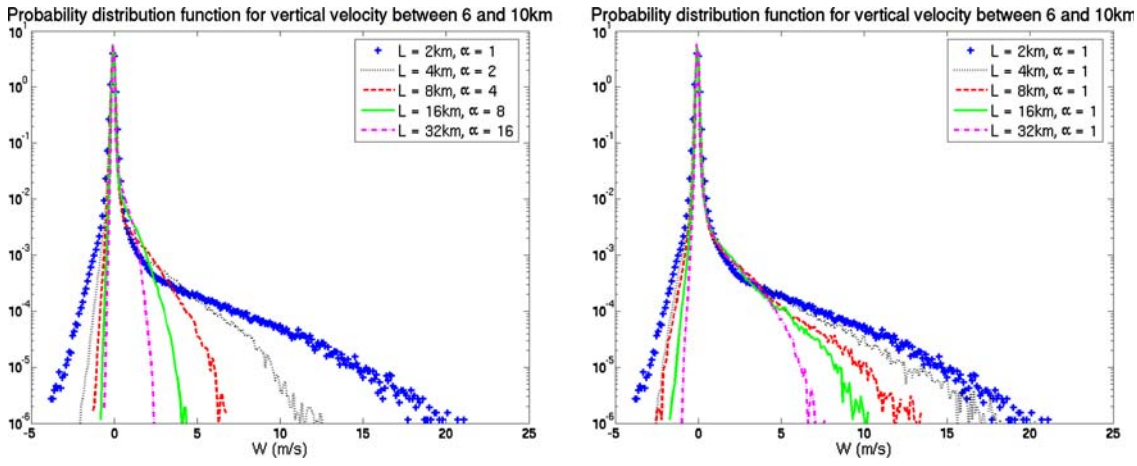

Fig. 6 Vertical velocity probability distribution function between 6 and 10 km in the strong-shear experiment. *Left panel*: hypohydrostatic runs, *right panel*: coarse-resolution runs

(31), implies

$$w_{\mathrm{cnv}}(\alpha\Delta x, \alpha) \approx \alpha^{-1} w_{\mathrm{cnv}}(\Delta x, 1), \tag{39}$$

where $w_{\mathrm{cnv}}(\Delta x, \alpha)$ is the convective velocity for a resolution Δx and rescaling parameter α. An implicit assumption in (39) is that the buoyancy in the updraft is independent of α.

The vertical velocity is significantly larger in the coarse-resolution runs. In fact, even for a resolution of 16 km, the strongest updrafts remain half as strong as in the $\Delta x = 2$ km reference case. Pauluis and Garner [15] analyze the impact of horizontal resolution on vertical velocity, and obtain a scaling for the vertical velocity as

$$w_{cnv}(\Delta x, 1) \approx \left(1 + \frac{\Delta x}{\Delta Z}\right)^{-\frac{1}{2}} w_{\mathrm{cnv},0}. \tag{40}$$

The scaling is similar to that of the ascent of an anisotropic bubble of diameter Δx and height ΔZ, with $w_{\mathrm{cnv},0}$ the velocity of an infinitely narrow bubble. As for (39), this scaling requires the buoyancy in the updraft to be independent of the model resolution. The parameter ΔZ in the scaling can be interpreted as the vertical extent of the convective updraft. Pauluis and Garner [15] found that $\Delta Z \approx 6$ km in their simulation of radiative-convective equilibrium in the absence of shear. The same value $\Delta Z \approx 6$ km works well for the weak shear case. For the strong shear, using $\Delta Z \approx 4$ km gives a better fit and also indicates a higher sensitivity to horizontal resolution. The lower value of ΔZ might be interpreted as a result of the strong shear tilting the updraft and reducing their vertical extent.

The scalings for vertical velocity (39) and (40) exhibit a higher sensitivity for the hypohydrostatic runs than for the coarse runs. Figure 7 compares the scalings with the third moment of vertical velocity obtained from the simulations. (The third moment is indicative of the production and dissipation of vertical kinetic energy. The second moment exhibits a similar behavior.) This confirms a very large reduction of the vertical velocity in the hypohydrostatic simulations, while the coarse-resolution runs are more robust. However, the hypohydrostatic simulations are less sensitive than predicted by the scaling (39). A possible explanation is the fact that the buoyancy in the convective updraft increases at large value of α to compensate partially for the hypohydrostatic slowdown.

4 Discussion

In hypohydrostatic rescaling, the inertia for vertical motion is artificially increased. This results in a slowdown of convective motions, combined with an increase in their horizontal scale, without affecting the large-scale hydrostatic dynamics of the atmosphere. As such, the hypohydrostatic rescaling offers a consistent method to reduce the scale separation between convection and the planetary scales. It has also been shown that, for a dry atmosphere, the hypohydrostatic rescaling is mathematically equivalent to both DARE and Deep Earth approaches. In DARE, the scale separation is reduced by shrinking and speeding up the planetary scales, while

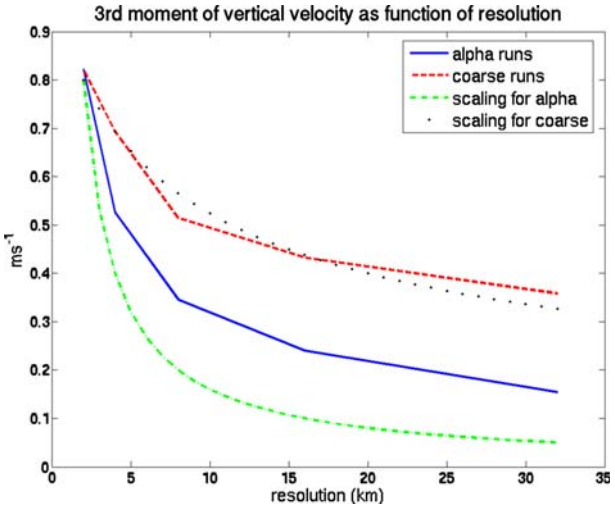

Fig. 7 Vertical velocity as function of the grid resolution in the strong-shear experiment. *Solid blue line* third moment for vertical velocity in the α runs. *Solid red line* the same for the coarse runs. *Dashed blue line* scaling (39) for the α runs. *Dashed red line* scaling (40) for the coarse runs

leaving the convective scales unchanged. In Deep Earth, the scale height of the atmosphere is increased by reducing the gravitational acceleration. This increases the convective scales without affecting the hydrostatic dynamics. These latter two approaches have the advantage that they are based on a physical analog rather than a mathematical modification of the equations. In practice however, implementing the hypohydrostatic rescaling is usually easier in numerical models, as it only requires changes to a single equation.

The hypohydrostatic rescaling should be viewed primarily as a tool to develop a new generation of global cloud-resolving atmospheric models. On a theoretical level, a key issue is to determine the effects of inadequate model resolution. This is essentially a problem of numerical convergence with a complex set of nonlinear partial differential equations. This problem can be recast through the hypohydrostatic rescaling into the question of determining the sensitivity of a fully resolved model as the rescaling parameter approaches unity. Hence, the issue of numerical convergence can be transformed into a question of physical behavior. From a modeling point of view, the hypohydrostatic rescaling reduces the scale separation between the convective and planetary scales. This makes it possible to use and develop global cloud-resolving models even with current computing resources. This can be used to compare global models with parameterized and explicit convection.

It is also important to determine whether the behavior of hypohydrostatic convection is sufficiently similar to atmospheric convection to replace traditional convective parameterization in global models. In the numerical simulations presented in this paper, simulations with small value of the rescaling parameter are able to reproduce the statistical behavior of convection, but large values significantly decreased the quality of the simulations. More importantly, these results also indicate that for the same computational cost, coarse-resolution simulations do a better job at reproducing the statistical behavior of convection, particularly for the cloud ice and vertical velocity distributions. Indeed, the scaling law for vertical velocity in coarse simulations obtained by Pauluis and Garner [15] indicates that the vertical velocity in deep convection is less sensitive to model resolution than to the hypohydrostatic rescaling parameter. Hence, as far as practical application are concerned, coarse-resolution models are likely to offer a superior alternative to the hypohydrostatic rescaling.

Whether rescaling or coarse-resolution simulations offer an answer to the problem of the representation of convection in climate models depends crucially on whether they can capture the interaction between the large-scale circulation and convection. The discussion in this paper has primarily focused on the behavior at the convective scale, while a companion paper [5] investigates the planetary scale. The fundamental question here remains: to understand the behavior of the atmosphere at the intermediary scales. While this issue is left for a future paper, it should be pointed out here that the slowdown of convection by the hypohydrostatic rescaling implies a much slower convective adjustment. This is most likely the main limitation of the use of the hypohydrostatic rescaling for simulations of the Earth's atmosphere. Indeed, the reduction in the spatial scale separation is also associated with a reduction in the time-scale separation: rescaled convective motions become slower compared to the large-scale dynamics. The slower behavior of convection would modify the way it interacts with its large-scale environment. The convective adjustment time for deep convection, i.e. the

time it takes to remove convective instability, lies between 2 and 24 h. Only relatively small values – less than 10 – of the rescaling parameter can be used before this convective time scale becomes comparable to that of synoptic motions.

Appendix: Turbulent closure under the hypohydrostatic rescaling

A turbulent kinetic energy (TKE) scheme is used in the Zetac model to determine the sub-grid-scale momentum, energy and water vapor fluxes. A prognostic equation for the TKE is given by

$$\frac{\mathrm{dTKE}}{\mathrm{d}t} = \overline{w'b'} - D - \overline{u'v'}\frac{\partial u}{\partial y} - \overline{u'v'}\frac{\partial v}{\partial x} - \overline{u'w'}\frac{\partial w}{\partial x} - \overline{u'w'}\frac{\partial u}{\partial z} - \overline{v'w'}\frac{\partial v}{\partial z} - \overline{v'w'}\frac{\partial w}{\partial y} - \overline{u'^2}\frac{\partial u}{\partial x} - \overline{v'^2}\frac{\partial v}{\partial y} - \overline{w'^2}\frac{\partial w}{\partial z} \tag{41}$$

Here, u, v, and w are the velocity at the resolved scale, and u', v' and w' are the sub-grid-scale velocity. The overline indicates averaging over a grid box, so $\mathrm{TKE} = \frac{1}{2}(\overline{u'^2} + \overline{v'^2} + \overline{w'^2})$. The first term on the right-hand side is the production of TKE due to sub-grid-scale flux of buoyancy, which depends on the potential temperature flux, humidity flux and on whether the environment is saturated. The second term D is the dissipation of TKE by the turbulent energy cascade. The remaining terms represent the conversion of kinetic energy at the resolved scale into TKE.

Under the hypohydrostatic rescaling, the kinetic energy becomes $\mathrm{ke} = \frac{1}{2}(u^2 + v^2 + \alpha^2 w^2)$. Leaving equation (41) unchanged would result in an inconsistency between the resolved and unresolved kinetic energy, which can produce an artificial source of kinetic energy. In early test simulations with $\alpha = 8$ and $\alpha = 16$, this lead to a destabilization of convective updrafts. A consistent treatment of the turbulent closure can be obtained by redefining the TKE in the hypohydrostatic rescaling as $\mathrm{TKE}_\alpha = \frac{1}{2}(\overline{u'^2} + \overline{v'^2} + \overline{\alpha^2 w'^2})$. In this case, the prognostic equation for TKE becomes

$$\frac{\mathrm{dTKE}_\alpha}{\mathrm{d}t} = \overline{w'b'} - D - \overline{u'v'}\frac{\partial u}{\partial y} - \overline{u'v'}\frac{\partial v}{\partial x} - \overline{u'w'}\frac{\partial u}{\partial z} - \alpha^2\overline{u'w'}\frac{\partial w}{\partial x} - \overline{v'w'}\frac{\partial v}{\partial z} - \alpha^2\overline{v'w'}\frac{\partial w}{\partial y} - \overline{u'^2}\frac{\partial u}{\partial x} - \overline{v'^2}\frac{\partial v}{\partial y} - \alpha^2\overline{w'^2}\frac{\partial w}{\partial z} \tag{42}$$

Under the hypohydrostatic approximation, the sub-grid-scale vertical velocity scales as $w' \sim \alpha^{-1}u'$. Similarly, the vertical extent of the eddies should be smaller than their horizontal size by a factor α. Hence, for the simulations discussed in this paper, the vertical diffusivity D_v have been rescaled as $\alpha^{-2}D_h$, where D_h is the horizontal diffusivity.

Acknowledgment We would like to thank Z. Kuang, P. Blossey, and C. Bretherton for the many insightful discussions on this topics.

References

1. Anderson, J.L., Balaji, V., Broccoli, A.J., Cooke, W.F., Delworth, T.L., Dixon, K.W., Donner, L.J., Dunne, K.A., Freidenreich, S.M., Garner, S.T., Gudgel, R.G., Gordon, C.T., Held, I.M., Hemler, R.S., Horowitz, L.W., Klein, S.A., Knutson, T.R., Kushner, P.J., Langenhorst, A.R., Lau, N.-C., Liang, Z., Malyshev, S.L., Milly, P.C.D., Nath, M.J., Ploshay, J.J., Ramaswamy, V., Schwarzkopf, M.D., Shevliakova, E., Sirutis, J.J., Soden, B.J., Stern, W.F., Thompson, L.A., Wilson, R.J., Wittenberg, A.T., Wyman, B.L.: The new GFDL global atmosphere and land model AM2/LM2: evaluation with prescribed SST simulations. J. Atmos. Sci **17**, 4641–4673 (2004)
2. Colella, P., Woodward, P.R.: The piecewise parabolic method (PPM) for gas-dynamical simulations. J. Comput. Phys. **54**, 174–201 (1984)
3. Davies-Jones, R.: An expression for effective buoyancy in surroundings with horizontal density gradients. J. Atmos. Sci. **60**, 2922–2925 (2003)
4. Freidenreich, S.M., Ramaswamy, V.: A new multiple-band solar radiative parameterization for general circulation models. J. Geophys. Res. **104**, 31, 389–31, 409 (1999)
5. Garner, S.G., Frierson, D., Held, I., Pauluis, O., Vallis, G.: Resolving convection in a global hypohydrostatic model. J. Atmos. Sci (2006) (submitted)

6. Grabowski W., Wu, X., Moncrieff, M.W.: Cloud-resolving modeling of tropical cloud systems during phase III of GATE. Part I: Two-dimensional experiments. J. Atmos. Sci. **53**, 3684–3709 (1996)
7. Grabowski, W., Yano, J.-I., Moncrieff, M.W.: Cloud resolving modeling of tropical circulations driven by large-scale SST gradients. J. Atmos. Sci. **57**, 2022–2040 (2000)
8. Held, I.M., Hemler, R.S., Ramaswamy, V.: Radiative-convective equilibrium with explicit two-dimensional moist convection. J. Atmos. Sci. **50**, 3909–3927 (1993)
9. Klemp, J.B., Wilhelmson, R.B.: The simulation of three-dimensional convective storm dynamics. J. Atmos. Sci. **35**, 1070–1096 (1978)
10. Krueger, S.K., Fu, Q., Liou, K.N., Schin, H.-N.: Improvements of an ice-phase microphysics parameterization for use in numerical simulations of tropical convection. J. Appl. Meteorol. **34**, 281–287 (1995)
11. Kuang, Z., Blossey, P.N., Bretherton, C.S.: A new approach for 3D cloud resolving simulations of large scale atmospheric circulation. Geophys. Res. Lett. **32**, L02809 (2005)
12. Lin, Y.-L., Farley, R.D., Orville, H.D.: Bulk parameterization of the snow field in a cloud model. J. Appl. Meteorol. **22**, 1065–1092 (1983)
13. Lipps, F.B., Hemler, R.S.: Scale analysis of deep, moist convection and some related numerical calculations. J. Atmos. Sci. **39**, 2192–2210 (2004)
14. Lord, S.J., Willoughby, H.E., Piotrowicz, J.M.: Role of a parameterized ice-phase microphysics in an axisymmetric, nonhydrostatic tropical cyclone model. J. Atmos. Sci. **41**, 2836–2848 (1984)
15. Pauluis, O., Garner, S.: Sensitivity of radiative-convective equilibrium simulations to horizontal resolution. J. Atmos. Sci. **63**, 1910–1923 (2006)
16. Pedlosky, J.: Geophysical Fluid Dynamics. Springer, Berlin Heidelberg New York, p. 728, 1979
17. Randall D., Krueger, S., Bretherton, C., Curry, J., Duynkerke, P., Moncrieff, M., Ryan, B., Starr, D., Miller, M., Rossow, W., Tselioudis, G., Wielicki, B.: Confronting models with Data: the GEWEX cloud systems study. Bull. Am. Meteorol. Soc. **84**, 455–469 (2003a)
18. Randall, D.A., Khairoutdinov, M., Arakawa, A., Grabowski, W.: Breaking the cloud parameterization deadlock. Bull. Am. Meteorol. Soc. **84**, 1547–1564 (2003b)
19. Tomita, H., Miura, H., Iga, S., Nasuno, T., Satoh, M.: A global cloud-resolving simulation: preliminary results from an aqua planet experiment. Geophys. Res. Lett. **32**, L08805. DOI:10.1029/2005GL022459 (2005)
20. Tompkins, A, Craig, G.C.: Radiative-convective equilibrium in a three-dimensional cloud-ensemble model. Q. J. R. Meteorol. Soc. **124**, 2073–2097 (1998)
21. Xu, K.-M., Randall, D.: Explicit simulation of cumulus ensembles with the GATE phase III data: comparison with observations. J. Atmos. Sci. **53**, 3710–3736 (1996)